The Journal of Immunology

Blockade of Notch1 Signaling Alleviates Murine Lupus via Blunting Macrophage Activation and M2b Polarization

Weijuan Zhang, Wei Xu and Sidong Xiong

J Immunol 2010; 184:6465-6478; Prepublished online 28 April 2010;
doi: 10.4049/jimmunol.0904016
http://www.jimmunol.org/content/184/11/6465

The Journal of Immunology is published twice each month by
The American Association of Immunologists, Inc.,
1451 Rockville Pike, Suite 650, Rockville, MD 20852

Print ISSN: 0022-1767 Online ISSN: 1550-6606.

Blockade of Notch1 Signaling Alleviates Murine Lupus via Blunting Macrophage Activation and M2b Polarization

Weijuan Zhang,* Wei Xu,* and Sidong Xiong*,†

Patients with systemic lupus erythematosus (SLE) are found to be accompanied with innate immunity dysregulation including abnormally macrophage activation. But the functional polarization of the activated macrophages and its underlying molecular mechanism during the pathogenesis of SLE remains unknown. As an important local cellular interaction mechanism responsible for cell fate determination, Notch signaling is reported to exert crucial functions in the development and differentiation of various immunocytes, whereas its role in macrophage polarization is not fully understood. In this study, in the SLE murine model generated by immunization with activated lymphocyte-derived DNA (ALD-DNA), infiltrated macrophages in the nephritic tissues were found to exhibit activation and M2b functional polarization. Notch1 signaling activity was significantly upregulated in the ALD-DNA–induced M2b macrophages in vitro and in vivo. Furthermore, ALD-DNA–induced M2b polarization was found to be dependent on enhanced Notch1 signaling through accelerating NF-κB p50 translocation into the nucleus mediated by PI3K and MAPK pathways. Moreover, blockade of Notch1 signaling with γ-secretase inhibitor treatment before or after the disease initiation could ameliorate murine lupus through impeding macrophage M2b polarization. Our results implied that Notch1 signaling-dependent macrophage M2b polarization might play a pivotal role in the pathogenesis of SLE, which could provide Notch1 signaling blockade as a potential therapeutic approach for SLE disease. ***The Journal of Immunology*****, 2010, 184: 6465–6478.**

Systemic lupus erythematosus (SLE) is a potentially fatal disease characterized by the prototypic autoimmune syndrome with heterogeneous manifestations frequently including autoimmunity, vasculitis, arthritis, and glomerulonephritis (1–4). Autoimmunity driving by self-DNA released during normal or pathological cell death that fails to be cleared from bloodstream has been reported to cause systemic autoimmune disease in both autoimmune-prone mice and nonautoimmune-prone mice (5–8). Through immunizing syngeneic female BALB/c mice with activated lymphocyte-derived DNA (ALD-DNA), we have established an SLE murine model that developed highly anti-dsDNA Abs, proteinuria, immune complex glomerular deposition, and glomerulonephritis (9, 10). Given the emblematical autoimmune syndrome in this SLE murine model, the ALD-DNA–immunized mice could be used as an ideal model to explore the immunological mechanism for the pathogenesis of SLE disease.

SLE syndrome is generally considered to be autoantibody-mediated systemic inflammation and tissue damage triggered by aggressive T and B cell responses of the adaptive immune system (11, 12). Yet, the underlying cellular and molecular mechanisms for onset and progression of SLE are still poorly understood (13). It was reported that markedly activated macrophages and other myeloid cells that infiltrated lymphoid tissues and kidneys mediated the onset and propagation of an aggressive adaptive immune response, thereby leading to SLE pathogenesis in mice (13–15). Accumulating data demonstrated that F4/80$^+$ macrophages represented the major inflammatory infiltrated cells and played a crucial pathogenic role in the development of SLE nephritis (13–19).

Macrophages display remarkable plasticity and can change their physiology in response to exposure to various microenvironmental signals (20, 21). These changes, also termed as functional macrophage polarization, can give rise to different populations of cells with diverse gene expression profiles and distinct functions (22, 23). Functional macrophage polarization represents different extremes of a continuum ranging from M1, M2a, and M2b to M2c (24). M1 polarization, driven by IFN-γ and LPS, typically acquires fortified cytotoxic and antitumoral properties, whereas M2 polarization generally obtains immunoregulatory and protumoral activities (25, 26). In particular, M2a polarization, induced by IL-4 and IL-13, and M2b polarization, induced by combined immune complexes with TLR or IL-1R agonists, exert immunoregulatory functions and drive type II responses, whereas M2c polarization, induced by IL-10, gains immunosuppression and tissue-remodeling activities (24). Although the critical role of macrophage activation in the pathogenesis of SLE has been validated, the concrete phenotype and mechanism for functional macrophage polarization in SLE remains unclear.

As an evolutionarily conserved local cell-interaction mechanism controlling cell specification, Notch signaling is critical for T/B cell lineage determination during hematopoiesis and immune development (27–29). Notch signaling was also found to participate in cell fate decision of monocytes and functional modulation of macrophages (30, 31). Enhanced Notch1 signaling on macrophages induced by TLRs and other various stimuli could regulate macrophage function, including cytokine producing ability, Ag-presenting capacity, and cytotoxic activity (32–34). Furthermore,

*Institute for Immunobiology and Department of Immunology, Shanghai Medical College, Fudan University, Shanghai; and †Institute of Biology and Medical Sciences, Soochow University, Suzhou, People's Republic of China

Received for publication December 14, 2009. Accepted for publication March 25, 2010.

This work was supported by grants from the National Natural Science Foundation of China (30890141, 30671952), Major State Basic Research Development Program of China (2007CB512401), and Program for Outstanding Medical Academic Leader of Shanghai (LJ06011, 07JC14004).

Address correspondence and reprint requests to Dr. Sidong Xiong, Institute for Immunobiology, Fudan University, 138 Yi Xue Yuan Road, Shanghai 200032, People's Republic of China. E-mail address: sdxiongfd@126.com

The online version of this article contains supplemental material.

Abbreviations used in this paper: ALD-DNA, activated lymphocyte-derived DNA; BM, bone marrow; BMDM, bone marrow-derived macrophage; DAPT, *N*-[*N*-(3,5-difluorophenacetyl)-L-alanyl]-*S*-phenylglycine t-butyl ester; GSI, γ-secretase inhibitor; iNOS, inducible NO synthase; IL-1ra, IL-1R antagonist; MR, mannose receptor; Notch1^{IC}, Notch1 intracellular domain; SLE, systemic lupus erythematosus; UnALD-DNA, unactivated lymphocyte-derived DNA.

Notch1 signaling could also regulate TLR responses in macrophages through integration with the IFN-γ pathway (31). In this sense, Notch1 signaling participates prodigiously in the modulation of macrophage activation and function. But its role in the abnormal macrophage functional polarization during the pathogenesis of SLE is scarcely documented.

In this study, we used a well-characterized murine model of SLE that depends on s.c. immunization of ALD-DNA to investigate the role of dysfunctional macrophage activation in the pathogenesis of SLE. We found that infiltrated macrophages in the nephritic tissues exhibited activation and M2b functional polarization, which was dependent on Notch1 signaling activation induced by ALD-DNA. More importantly, blockade of Notch1 signaling with γ-secretase inhibitor (GSI) treatment before or after disease initiation could mitigate SLE syndrome through blunting macrophage M2b polarization in the murine model. These results indicated that dysregulated macrophage activation and M2b polarization dependent on enhanced Notch1 signaling would mediate the initiation and progression of SLE disease, which might provide Notch1 signaling as a novel therapeutic target for patients with SLE.

Materials and Methods

Mice

Six- to 8-wk-old female BALB/c mice were purchased from the Experimental Animal Center of Chinese Academy of Sciences (Shanghai, People's Republic of China). Mice were housed in a specific pathogen-free room under controlled temperature and humidity. All mice procedures were conducted according to the Guide for the Care and Use of Medical Laboratory Animals (Ministry of Health, People's Republic of China, 1998) and with the ethical approval of the Shanghai Medical Laboratory Animal Care and Use Committee as well as the Ethical Committee of Fudan University (Shanghai, People's Republic of China).

Cell culture

RAW264.7 cells were cultured in RPMI 1640 (Invitrogen, Carlsbad, CA) supplemented with 2 mM glutamine and 10% FBS (Invitrogen) in a 5% CO_2 incubator at 37˚C. For generation of bone marrow-derived macrophages (BMDMs), BM cells were harvested from uninfected, normal BALB/c mice and filtered through nylon mesh. BM cells were cultured in L929 cell-conditioned medium at a density of 3×10^5 cells/ml medium and maintained in a 5% CO_2 incubator at 37˚C as described previously (25, 35). Six days after initial BM cell culture, the medium was changed, and the purity of $F4/80^+$ cells was >90%, as determined by flow cytometry.

Plasmid construction and cell transfection

To construct the MSCVpac-FLAG-$Notch1^{IC}$ plasmid encoding for Notch1 intracellular domain ($Notch1^{IC}$), the full-length of $Notch1^{IC}$ cDNA was amplified from total RNA of HepG2 cells using the primers 5′-CCG GGT CGA CGC ACC ATG GCA CGC AAG CGC CGG CGG CAG-3′ and 5′-GCG ACG CGG CCG CCT TGA AGG CCT CCG AAT-3′ and cloned into the SalI and NotI sites of the MSCVpac-FLAG retroviral vector kindly provided by Prof. Tadatsugu Taniguchi (University of Tokyo, Tokyo, Japan). PA317 cells were cultured in DMEM (Invitrogen) supplemented with 10% FBS on a 100-mm dish at a concentration of 2×10^5 cells/ml for 24 h and transfected with the MSCVpac-FLAG-$Notch1^{IC}$ plasmid by electroporation as described previously (36, 37). The culture supernatants of transfected PA317 cells were harvested and stored at −70˚C. RAW264.7 cells were infected with the retrovirus from the culture supernatants for 48 h, and then selected with 3.0 μg/ml puromycin (AMRESCO, Solon, OH) for stable $Notch1^{IC}$ expression clones.

DNA preparation

ALD-DNA and unactivated lymphocyte-derived DNA (UnALD-DNA) were prepared with murine splenocytes that were generated from surgical resected spleens of 6- to 8-wk-old female BALB/c mice and cultured with or without Con A (Sigma-Aldrich, St. Louis, MO) in vitro (9, 10). For generation of ALD-DNA, splenocytes were seeded at 2×10^6 cells/ml in a 75 cm^2 cell-culture flask and cultured in the presence of Con A (5 μg/ml) for 6 d to induce apoptosis. The apoptotic cells were stained with FITC-labeled Annexin V (BD Biosciences, San Jose, CA) and propidium iodide (Sigma-Aldrich), and sorted using an FACSAria (BD Biosciences). Genomic DNAs from syngeneic apoptotic splenocytes were treated with S1 nuclease (Takara Bio, Shiga, Japan) and proteinase K (Sigma-Aldrich), and then purified using the DNeasy Blood and Tissue Kits (Qiagen, Valencia, CA) according to the manufacturer's instructions. UnALD-DNA was prepared with unactivated (resting) splenocytes and extracted using the same methods. To exclude contaminations with LPS, sterile endotoxin-free plastic ware and reagents were used for DNA preparation. DNA samples were also monitored for low level of endotoxin by the *Limulus* amoebocyte lysate assay (BioWhittaker, Walkersville, MD) according to the manufacturer's instructions. The concentration of DNA was determined by detection of the absorbance at 260 nm. The apoptotic DNA ladder of ALD-DNA was confirmed by agarose gel electrophoresis.

Generation of SLE murine model

To generate the SLE murine model, 6- to 8-wk-old female BALB/c mice were immunized s.c. with ALD-DNA (50 μg/mouse) plus CFA (Sigma-Aldrich) on day 1, followed by s.c. injection of ALD-DNA (50 μg/mouse) emulsified with IFA (Sigma-Aldrich) on days 14 and 28 for total of three times as described previously (9, 10). Serum and urine samples were collected every 2 wk for further experiments. Eight weeks later, mice were sacrificed, and surgical resected spleens and kidneys were collected for further cellular function and tissue histology analysis.

Autoantibody and proteinuria examination

Anti-dsDNA Abs in the mice serum were determined by ELISA assay. ELISA plates (Costar, Cambridge, MA) were pretreated with protamine sulfate (Sigma-Aldrich) and then coated with calf thymus dsDNA (Sigma-Aldrich). Post-incubation with mouse serum, the levels of anti-dsDNA Abs were detected with the HRP-conjugated goat anti-mouse IgG and IgM (Southern Biotechnology Associates, Birmingham, AL). Tetramethylbenzidine substrate was used to develop colors, and absorbance at 450 nm was measured on a microplate reader (Bio-Tek ELX800, Bio-Tek Instruments, Winooski, VT). Avidity of anti-dsDNA IgG in serum was determined using ELISA with urea elution step as previously described (38). Proteinuria of the mice was measured with the BCA Protein Assay Kit (Thermo Fisher Scientific, Waltham, MA) according to the manufacturer's instructions.

Flow cytometry analysis and cell sorting

Murine renal tissues were surgical resected and dispersed in RPMI 1640 containing 5% FBS and 0.1% collagenase (Sigma-Aldrich) at 37˚C for 30 min, followed by progressive sieving to obtain single-cell suspensions. Single-cell suspensions of the murine splenic tissues were also prepared. To analyze gene expression in the renal macrophages, $CD11b^+/F4/80^{high}$ renal macrophages were sorted from nephritic single-cell suspensions using a FACSAria (BD Biosciences) with FITC-labeled anti-F4/80 and PE-labeled anti-CD11b (BD Biosciences). To analyze cytokine and Ab production in vitro, $CD4^+$ T cells and $CD19^+$ B cells were sorted from splenic single-cell suspensions by FACS using FITC-labeled anti-CD4 and PE-labeled anti-CD19 (BD Biosciences). The purity of isolated cells was confirmed at >90%. To assess the expression of activation and other biological markers on macrophages, flow cytometry analysis was performed with FITC- or PE-labeled anti-MHC class II, FITC-labeled anti-CD40, PE-labeled anti-CD80, PE-labeled anti-CD86, and PE-labeled anti-mannose receptor (MR; CD206) (BD Biosciences). To assess inducible NO synthase (iNOS) and $Notch1^{IC}$ expression in macrophages, the cells were stained for surface markers with FITC-labeled anti-F4/80 and resuspended in fixation/permeabilization solution (BD Cytofix/Cytoperm Kit, BD Biosciences), then stained with PE-labeled anti-iNOS (Santa Cruz Biotechnology, Santa Cruz, CA) and PE-labeled anti-Notch1 (eBioscience, San Diego, CA), respectively. To detect the expression and phosphorylation levels of p38 MAPK, Akt, and ERK1/2 in macrophages, flow cytometry analysis was performed with anti-p38 MAPK, anti-phospho-p38 MAPK (Thr180/Tyr182), anti-Akt, anti-phospho-Akt (Ser473), anti-ERK1/2, anti-phospho-p44/42 MAPK/ERK (Thr202/Tyr204) (Cell Signaling Technology, Beverly, MA), and FITC-labeled anti-IgG (eBioscience) as described previously (39). All flow cytometry data were acquired on an FACSCalibur (BD Biosciences) in CellQuest (BD Biosciences) and analyzed by FlowJo software (Tree Star, Ashland, OR).

Arginase assay

Arginase activity was analyzed as described previously (40). Briefly, macrophages were lysed with 0.1% Triton X-100. Lysates were combined with 12.5 mM Tris-HCl and 1 mM $MnCl_2$. Arginase was activated by heating for 10 min at 56˚C, and L-arginine substrate was added to 250 mM final concentration. Reactions were incubated at 37˚C for 30 min and stopped by the addition of H_2SO_4/H_3PO_4. Postaddition of α-isonitrosopropiophenone and

heating for 30 min at 95°C, urea production was measured by absorbance at 540 nm and normalized to cell counts.

Real-time PCR analysis

Total RNA was isolated from cultured cells or mouse renal macrophages with TRIzol reagent (Invitrogen) and was reverse transcribed using a cDNA synthesis kit (Fermentas, Burlington, Ontario, Canada) according to the manufacturer's instructions. Subsequently, cDNA was subjected to quantitative real-time PCR using a Lightcycler480 and SYBR Green system (Roche Diagnostic Systems, Somerville, NJ) following the manufacturer's protocol. The primer sequences used in this study are provided in Supplemental Table I.

ELISA assay

To assess protein levels of TNF-α, IL-1β, IL-4, IL-6, IL-10, IL-12, and MCP-1 in the cell culture supernatants, ELISA assays were performed with relative ELISA Kits (eBioscience) according to the manufacturer's instructions.

Western blot analysis

Whole, cytoplasmic, and nuclear protein extraction and Western blot analysis were performed as described previously (41, 42). Abs used here were anti-GAPDH (Santa Cruz Biotechnology), anti–β-actin (Santa Cruz Biotechnology), anti-cleaved Notch1 (Cell Signaling Technology), anti–NF-κB p50 (Millipore, Bedford, MA), anti–NF-κB p65 (Millipore), goat anti-mouse IgG-HRP (Santa Cruz Biotechnology), and goat anti-rabbit IgG-HRP (Santa Cruz Biotechnology).

Phagocytosis assay

ALD-DNA was labeled with Alexa Fluor 488 (Invitrogen) according to the manufacturer's instructions. The labeled ALD-DNA (referred as AF488-ALD-DNA) was purified using Bio-Rad Micro Bio-Spin P-30 column (Bio-Rad, Hercules, CA) according to the manufacturer's protocol. BMDMs were pretreated with *N*-[*N*-(3,5-difluorophenacetyl)-L-alanyl]-*S*-phenylglycine t-butyl ester (DAPT) or DMSO for 1 h and incubated with Alexa Fluor 488-labeled ALD-DNA for 2 h at 37°C as described previously (43). Phagocytosis of Alexa Fluor 488-labeled ALD-DNA was assessed by flow cytometry (FACSCalibur, BD Biosciences).

GSI treatment

The GSI DAPT (Sigma-Aldrich) was dissolved with DMSO (Sigma-Aldrich) for 10 mM additive stock solution or dissolved with 100% ethanol for 5 mg/ml gavage stock solution. DAPT additive stock solution or vehicle control DMSO (final concentration 1:1000) was added to the cultured macrophages 1 h before ALD-DNA stimulation. DAPT gavage solution or vehicle control gavage solution was prepared freshly by combination DAPT stock solution or 100% ethanol with corn oil (Sigma-Aldrich) at a ratio of 95% corn oil:5% ethanol. To analyze the effect of GSI treatment on the onset of nephritis and macrophage activation, 6- to 8-wk-old female BALB/c mice were randomized to feed with DAPT gavage solution or vehicle control gavage solution at 5 mg/kg per day for 3 mo. Twenty-four hours after the initial DAPT or vehicle control gavage solution treatment, the mice were immunized with ALD-DNA (50 μg/mouse), UnALD-DNA (50 μg/mouse), or PBS three times in 4 wk as previously described. Eight weeks after initial immunization, mice were sacrificed, and surgical resected spleens and kidneys were collected for further cellular function and tissue histology analysis. To analyze the effect of GSI treatment on the established nephritis and macrophage activation, 6- to 8-wk-old female BALB/c mice were immunized with ALD-DNA (50 μg/mouse), UnALD-DNA (50 μg/mouse), or PBS three times in 4 wk. Six weeks after initial immunization, the mice were randomized to feed with DAPT gavage solution or vehicle control gavage solution at 5 mg/kg per day for 6 wk. Twelve weeks after initial immunization, mice were sacrificed, and surgical resected spleens and kidneys were collected for further cellular function and tissue histology analysis. Serum and urine samples of the mice were collected every 2 wk.

Histology

Murine renal tissues were surgical resected and fixed in 4% paraformaldehyde (Sigma-Aldrich), processed, and embedded in paraffin. H&E staining of renal tissue sections were performed according to the manufacturer's instructions and assessed by a pathologist blinded to treatment group. The kidney score of glomerulonephritis was determined by using the ISN/RPS2003 classification. Fluorescent staining of cryosections was used for autoantibody deposition analysis in the glomeruli. Sections were fixed in acetone for 10 min and incubated with FITC-conjugated goat anti-mouse IgG (H+L chain-specific) Ab (Sigma-Aldrich) for 30 min. Pictures were acquired with a 20×/0.45 Plan Fluor object on a Nikon SCLIPSS TE2000-S microscope (Nikon, Melville, NY) equipped with ACT-1 software (Nikon). Original magnification was ×200.

Statistical analysis

The experimental data in this study were presented as the means ± SD of three independent experiments or from a representative experiment of three independent experiments. The statistical significance of the differences in the experimental data were valued by the Student *t* test. The statistical significance level was set as $*p < 0.05$; $**p < 0.01$; $***p < 0.001$.

Results

ALD-DNA immunization leads to macrophage infiltration and M2b polarization in SLE murine renal tissues

Although studies on SLE often focus on T and B lymphocytes, APCs such as macrophages might play vital roles in the pathogenesis of the disease (11). To explore the role of macrophages during pathogenesis of glomerulonephritis in an SLE murine model generated by immunizing female BALB/c mice with ALD-DNA, nephritic lymphocytes were extracted and analyzed for the presence of F4/80$^+$ cells. F4/80$^+$ cells were remarkably increased in the renal tissues of the SLE mice (Fig. 1*A*). Real-time PCR analysis for inflammatory gene expression showed that the purified renal macrophages from the SLE mice exhibited enhanced *IL-10*, *TNF-α*, *IL-1β*, *IL-6*, *MCP-1*, and *Nos2* (*iNOS*) but low *IL-12*, *TGF-β*, *IL-1R antagonist* (*IL-1ra*), and *arginase 1* (*Arg1*) mRNA levels, which displayed M2b (type II)-polarized phenotype (Fig. 1*B*, Table I). Renal macrophages from the SLE mice showed elevated expression of activation markers including MHC class II, CD80, CD86, and iNOS (Fig. 1*C*, 1*E*) but not MR expression and arginase activity (Fig. 1*C*, 1*D*) compared with those from control mice. Flow cytometry analysis of the surface markers showed that the renal macrophages from the SLE mice were also predominantly Ly6C^{low}, CD62L^{low}, and CD43$^{high/int}$ (Fig. 1*F*), which was consistent with previous reports on macrophage M2b polarization (11). Taken together, these data indicate that accumulating renal F4/80$^+$ macrophages displays an M2b-polarized phenotype in the SLE murine model.

Macrophages treated with ALD-DNA display the M2b phenotype in vitro

To further confirm that ALD-DNA stimulation could induce macrophage M2b polarization, BMDMs and RAW264.7 cells were stimulated with ALD-DNA in vitro. Enhanced MHC class II, CD80, and CD86 expression was observed in ALD-DNA–induced macrophages compared with those in control macrophages (Fig. 2*A*). Significantly higher levels of TNF-α, IL-1β, IL-6, IL-10, and MCP-1 but not IL-12 were produced in the supernatants of BMDMs and RAW264.7 cells stimulated with ALD-DNA compared with those of control macrophages (Fig. 2*B*, 2*C*). These data verify that macrophages treated with ALD-DNA show the M2b phenotype in vitro.

ALD-DNA stimulation upregulates Notch1 signaling in M2b macrophages

Previous reports indicated that Notch1 signaling contributed to macrophage activation (31, 32, 34). To determine the expression pattern of various Notch receptors on activated macrophages, real-time PCR was used to analyze *Notch1*, *-2*, *-3*, and *-4* mRNA levels. As shown in Fig. 3*A*, treatment of RAW264.7 cells with ALD-DNA increased the mRNA level of *Notch1* but not that of *Notch2*, *Notch3*, or *Notch4* in macrophages. Both flow cytometry and Western blot analysis for Notch1^{IC} protein level supported that ALD-DNA stimulation increased Notch1 signaling in a time-

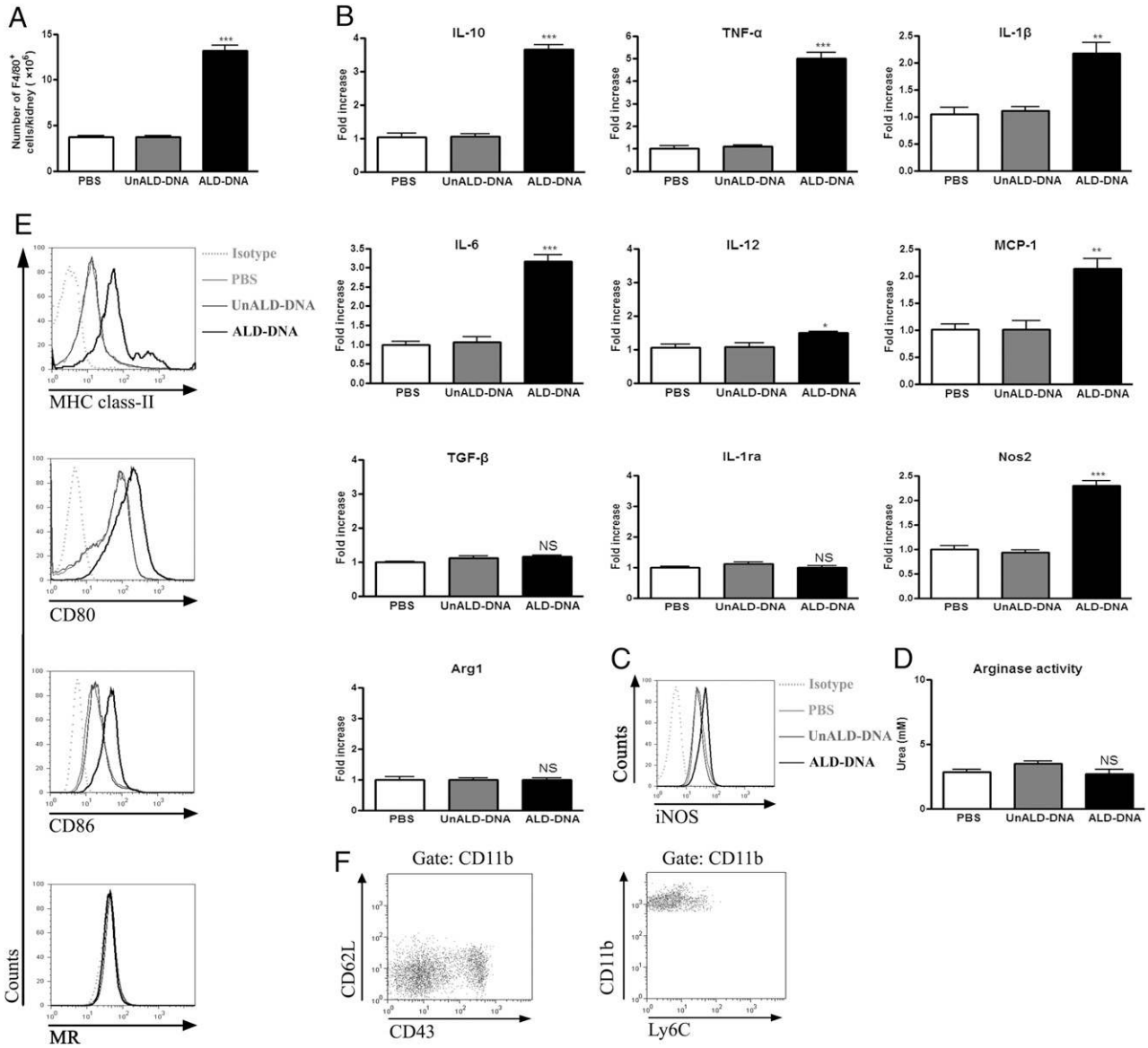

FIGURE 1. Significant increase of renal macrophage infiltration and M2b polarization in ALD-DNA–immunized SLE mice. Six- to 8-wk-old female BALB/c mice were immunized s.c. with ALD-DNA, UnALD-DNA, or PBS ($n = 10$) three times in 4 wk. *A*, The numbers of F4/80$^+$ cells per kidney in the renal tissues of the mice were determined by flow cytometry analysis. Data are means ± SD from 10 mice in each group. *B*, Cellular mRNA levels of *IL-10*, *TNF-α*, *IL-1β*, *IL-6*, *IL-12*, *MCP-1*, *TGF-β*, *IL-1ra*, *Nos2* (*iNOS*), and *arginase 1* (*Arg1*) in the CD11b$^+$/F4/80^{high} renal macrophages purified from mice were analyzed by real-time PCR. Data are means ± SD of three independent experiments. $n = 5$. *C*, Expression levels of iNOS in the renal F4/80$^+$ macrophages from the mice were determined by flow cytometry analysis. *D*, Arginase activity was assessed by an assay of urea production from arginine substrate and was normalized to cell counts. Data are means ± SD from 7–10 mice in each group. *E* and *F*, Expression levels of MHC class II, CD80, CD86, MR, Ly6C, CD62L, and CD43 in the renal macrophages from mice were determined by flow cytometry analysis. Data are representative of results obtained in three independent experiments with renal macrophages from five mice in each group. $*p < 0.05$; $**p < 0.01$; $***p < 0.001$.

and dose-dependent manner in activated macrophages in vitro (Fig. 3*B–E*) and in vivo (Fig. 3*F*). Furthermore, ALD-DNA stimulation increased series of Notch1 downstream genes such as *Hes1* and *Hey1* mRNA levels in a time- and dose-dependent manner in activated RAW264.7 cells in vitro (Fig. 3*G*). Taken together, ALD-DNA stimulation significantly increases the gene expression profile of the Notch1 signaling pathway in the M2b macrophages in vitro and in vivo.

GSI treatment blunts ALD-DNA–induced M2b polarization

To evaluate the role of Notch1 signaling in ALD-DNA–induced M2b polarization, we assessed macrophage functional activity after

Table I. *Functional properties of different polarized macrophages*

	M1	M2a	M2b	M2c
Secretory products	IL-12^{high}, TNF-α, IL-6, IL-1β	IL-10, IL-1ra	IL-10^{high}, IL-12^{low}, TNF-α, IL-1β, IL-6	IL-10, TGF-β
Biological markers	MHC class II, CD86, MR	MHC class II, MR	MHC class II, CD86	MR
Arginine metabolism	iNOS	Arg1	iNOS	Arg1

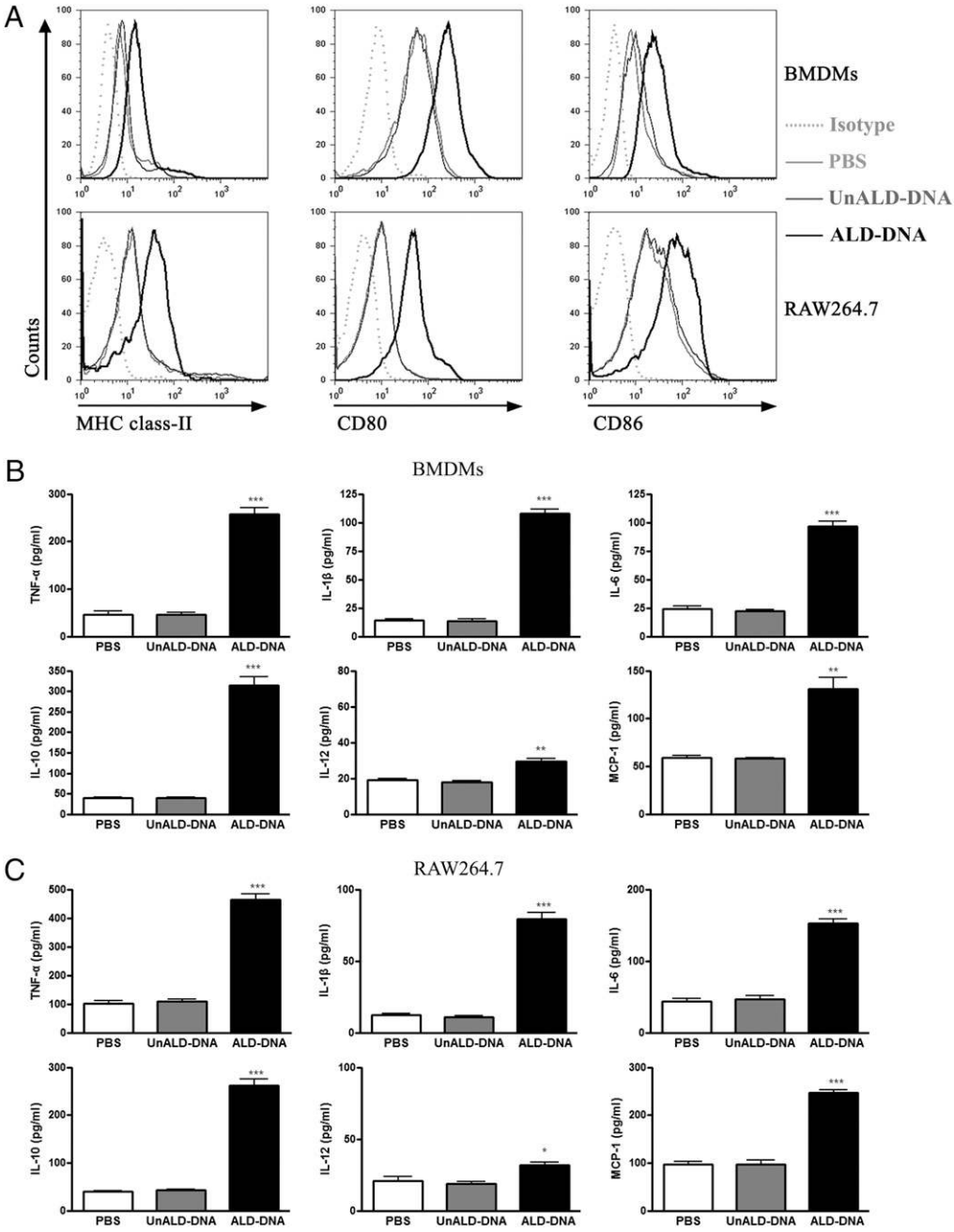

FIGURE 2. ALD-DNA induces macrophage M2b polarization in vitro. BMDMs and RAW264.7 cells were simulated with ALD-DNA, UnALD-DNA, or PBS. *A*, Expression levels of MHC class II, CD80, and CD86 in the macrophages were assessed by flow cytometry analysis. Data are representative of results obtained in three independent experiments. *B* and *C*, Levels of TNF-α, IL-1β, IL-6, IL-10, IL-12, and MCP-1 in the supernatants of the macrophages were measured by ELISA assay. Data are means ± SD of three independent experiments. $*p < 0.05$; $**p < 0.01$; $***p < 0.001$.

inhibiting Notch1 signaling through GSI treatment combined with ALD-DNA stimulation. Flow cytometry and Western blot analysis for Notch1^{IC} expression showed that the GSI DAPT efficiently inhibited Notch1^{IC} expression (Fig. 4*A*, 4*B*). ELISA analysis for inflammatory markers showed remarkable decreased production of TNF-α, IL-6, IL-10, IL-12, and MCP-1 but no significant change the production of IL-1β in DAPT-treated RAW264.7 cells compared with those in control cells (Fig. 4*C*). Flow cytometry analysis of the surface activation markers revealed reduced expression of MHC class II, CD40, and CD86 but no significant change in expression of CD80 on DAPT-treated RAW264.7 cells compared with those on control cells (Fig. 4*D*). Furthermore, phagocytosis assay showed that DAPT treatment had little effect on phagocytosis function of BMDMs (Fig. 4*E*). To evaluate the effect of decreased Notch1 signaling on the Ag-presenting ability of macrophages, we performed ELISA analysis for IL-4 and IL-10 production of CD4$^+$ T cells and anti-dsDNA Ab production of CD19$^+$ B cells cocultured with DAPT-treated BMDMs combined with ALD-DNA induction. It was found that not only IL-4 and IL-10 production by CD4$^+$ T cells, but also anti-dsDNA Abs production by B cells were severely decreased by coculturing with DAPT-treated BMDMs compared with control cells (Fig. 4*F*, 4*G*). Notch signaling was reported to be involved in regulating NF-κB activity (44, 45). Western blot analysis for NF-κB p50 and p65 after GSI treatment showed decreased NF-κB p50 translocation but intact NF-κB p65 translocation into the nucleus (Fig. 4*H*). These data indicate that blockade of the Notch1 signaling pathway by GSI treatment blunts ALD-DNA–induced M2b polarization.

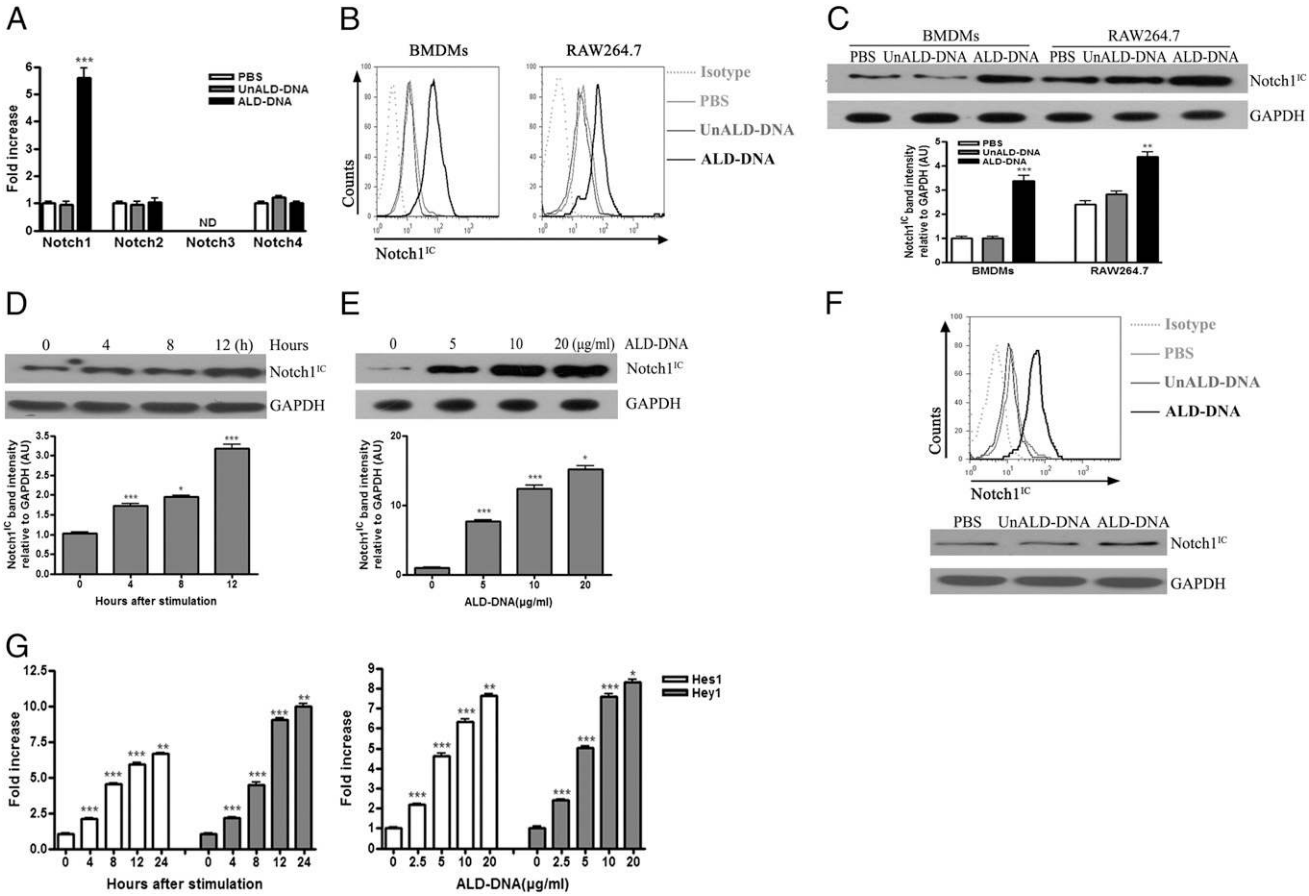

FIGURE 3. ALD-DNA treatment upregulates Notch1 signaling in M2b macrophages in vitro and in vivo. *A–C*, BMDMs and RAW264.7 cells were stimulated with ALD-DNA, UnALD-DNA, or PBS. *A*, mRNA levels of *Notch* receptors in the RAW264.7 cells were determined by real-time PCR. Data are means ± SD of three independent experiments. *B* and *C*, Protein expression levels of Notch1^{IC} in the macrophages were assessed by flow cytometry and Western blot analysis. Graphical representation of band intensities was shown in the picture below. Expression of Notch1^{IC} was normalized to GAPDH expression. *D* and *E*, Protein expression levels of Notch1^{IC} in the RAW264.7 cells stimulated with ALD-DNA (50 μg/ml) for the indicated time or with increasing amounts of ALD-DNA for 12 h were measured by Western blot analysis. Graphical representations of band intensities were shown in the pictures below. Expression of Notch1^{IC} was normalized to GAPDH expression. Data in *B–E* are representative of results obtained in three independent experiments or means ± SD of three independent experiments. *F*, Protein expression levels of Notch1^{IC} in the renal macrophages isolated from the immunized mice were assessed by flow cytometry and Western blot analysis. Data are representative of results obtained in three independent experiments with renal macrophages from five mice in each group. *G*, mRNA levels of *Hes1* and *Hey1* in the RAW264.7 cells stimulated with ALD-DNA (50 μg/ml) for the indicated time or with increasing amounts of ALD-DNA for 12 h were determined by real-time PCR analysis. Data are means ± SD of three independent experiments. $*p < 0.05$; $**p < 0.01$; $***p < 0.001$.

Notch1^{IC} overexpression promotes ALD-DNA–induced M2b polarization

To investigate the effect of increased Notch1 signaling on ALD-DNA–induced macrophage polarization, stable Notch1^{IC}-expressing RAW264.7 (RAW-Notch1^{IC}) and control (RAW-Vector) cells were produced and stimulated with ALD-DNA. ELISA analysis for the production of inflammatory markers induced by ALD-DNA showed remarkably increased production of TNF-α, IL-6, IL-10, IL-12, and MCP-1 but no significant change production of IL-1β in RAW-Notch1^{IC} cells compared with those in control cells (Fig. 5*A*, 5*B*). Interestingly, RAW-Notch1^{IC} cells stimulated with 25 μg/ml ALD-DNA produced more cytokines than control cells stimulated with 50 μg/ml ALD-DNA (Fig. 5*B*). Furthermore, flow cytometry analysis for the expression of activation markers induced by ALD-DNA revealed obvious enhanced expression of MHC class II, CD40, and CD86 but no significant change in expression of CD80 on RAW-Notch1^{IC} cells compared with those on control cells (Fig. 5*C*). Taken together, these results suggest that increasing Notch1 expression could enhance ALD-DNA–induced macrophage polarization.

Notch1 signaling facilitates ALD-DNA–induced M2b polarization through PI3K and MAPK signaling pathways

In many cell types, Notch1 signaling-induced survival effects require activation of PI3K and MAPK signaling pathways (46–48). ELISA analysis for inflammatory marker production in RAW-Notch1^{IC} cells showed remarkably decreased production of TNF-α and IL-10 upon treatment with LY294002 (PI3K inhibitor), SB203580 (p38 MAPK inhibitor), U0126 (MEK1/2 inhibitor), or PDTC (NF-κB inhibitor) but no significant change of cytokine production upon treatment with JAK inhibitor I (Fig. 6*A*). Western blot analysis for NF-κB p50 posttreatment with the inhibitors of PI3K, p38 MAPK, MEK1/2, or NF-κB showed abrogated NF-κB p50 translocation into the nucleus (Fig. 6*B*). Furthermore, exposure of macrophages to ALD-DNA showed increased phospho-p38, phospho-Akt, and phospho-ERK in a Notch1-dependent manner (Fig. 6*C*). Flow cytometry analysis for the expression of phospho-p38, phospho-Akt, and phospho-ERK in RAW-Notch1^{IC} cells revealed that PI3K inhibitor treatment abrogated the enhanced expression of phospho-Akt and phospho-ERK but had no significant effect on the expression of phospho-p38, whereas p38 MAPK

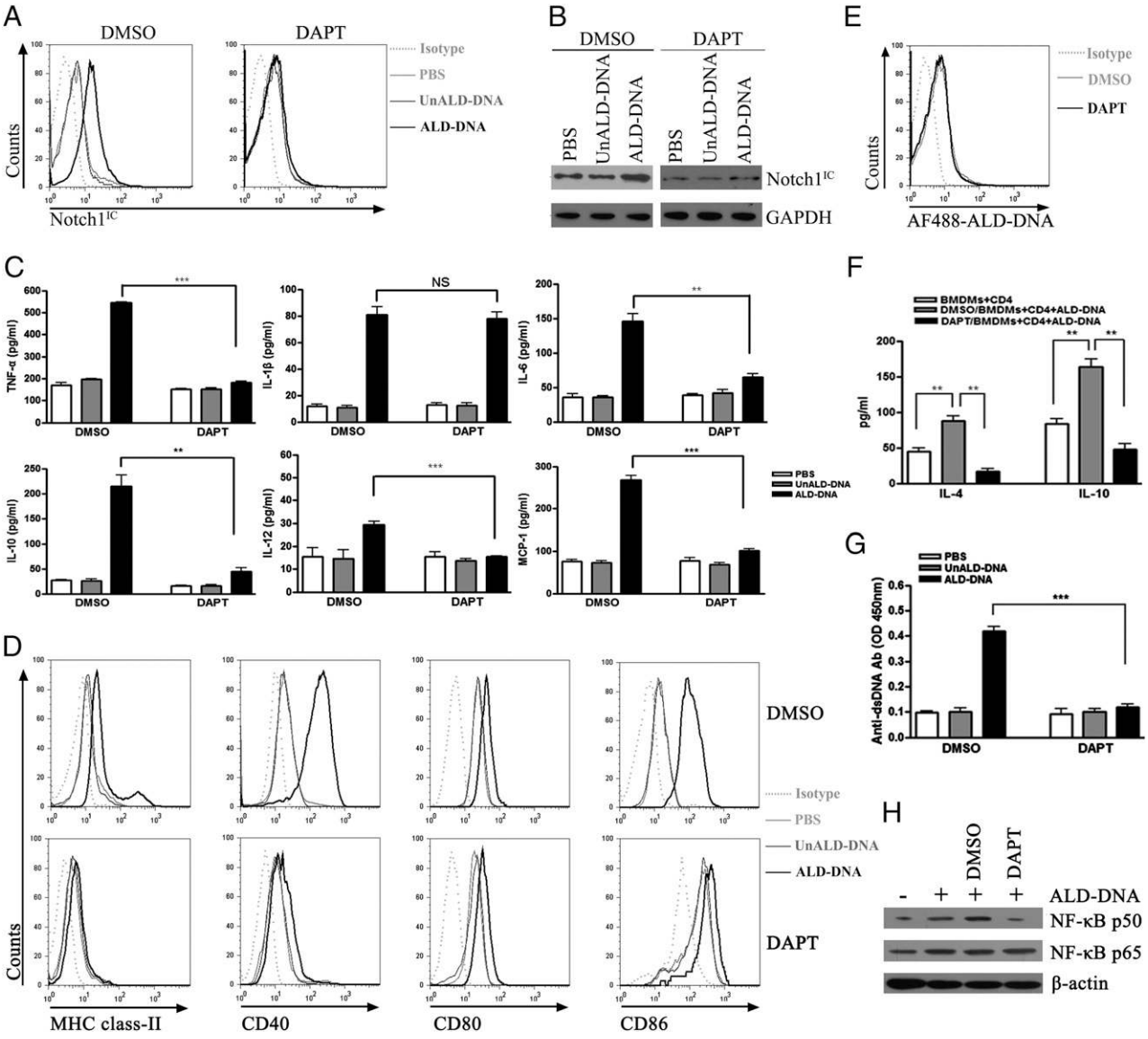

FIGURE 4. GSI treatment impairs ALD-DNA–induced M2b polarization. *A–E* and *H*, BMDMs and RAW264.7 cells were pretreated with DAPT (10 μM) or DMSO (0.1%) for 1 h, and then exposed to ALD-DNA, UnALD-DNA, or PBS. *A* and *B*, Twenty-four hours poststimulation, expression levels of $Notch1^{IC}$ in the RAW264.7 cells were assessed by flow cytometry and Western blot analysis. Data in *A* and *B* are representative of results obtained in three independent experiments. *C*, Twelve hours poststimulation, levels of TNF-α, IL-1β, IL-6, IL-10, IL-12, and MCP-1 in the supernatants of the RAW264.7 cells were measured by ELISA assay. Data are means ± SD of three independent experiments. *D*, Twenty-four hours poststimulation, expression levels of MHC class II, CD40, CD80, and CD86 in the RAW264.7 cells were assessed by flow cytometry analysis. *E*, DNA uptake abilities of the BMDMs upon DAPT treatment were measured by phagocytosis assay. Data in *D* and *E* are representative of results obtained in three independent experiments. *F*, BMDMs were pretreated with DAPT (10 μM) for 24 h, cocultured with $CD4^+$ T cells isolated from the SLE mice at a BMDMs/$CD4^+$ ratio of 1:5, and stimulated with ALD-DNA (50 μg/ml) for 48 h. Cytokine expression levels of IL-4 and IL-10 in the culture supernatants were analyzed by ELISA assay. *G*, BMDMs were pretreated with DAPT (10 μM) for 24 h, cocultured with $CD4^+$ T cells and $CD19^+$ B cells isolated from the SLE mice, and stimulated with ALD-DNA (50 μg/ml) for 6 d. Anti-dsDNA IgG levels in the culture supernatants were evaluated by ELISA. Data in *F* and *G* are means ± SD of three independent experiments. $n = 4$. *H*, One hour poststimulation, protein levels of NF-κB p50 and p65 in the nuclear extracts of the RAW264.7 cells were analyzed by Western blot analysis. Data are representative of results obtained in three independent experiments. $^{**}p < 0.01$; $^{***}p < 0.001$.

inhibitor treatment abrogated the enhanced expression of phospho-p38 but had no significant effect on the expression of phospho-Akt and phospho-ERK (Fig. 6*D–F*). These results suggest that PI3K/Akt-ERK1/2 and p38 MAPK signaling pathways link elevated Notch1 signaling with activated NF-κB signaling in the process of ALD-DNA–induced macrophage M2b polarization.

GSI treatment in vivo blockades Notch1 signaling activity in ALD-DNA–stimulated macrophages

To confirm the effect of GSI treatment on Notch1 signaling activity in vivo, we purified renal macrophages from DAPT or vehicle control gavage-treated BALB/c mice followed by ALD-DNA stimulation in vitro. Flow cytometry analysis for $Notch1^{IC}$ expression showed decreased Notch1 signaling on macrophages from DAPT-treated mice compared with those from vehicle control-treated mice (Fig. 7*A*). Moreover, real-time PCR analysis for mRNA levels of Notch1 downstream target genes revealed severely decreased *Hes1* and *Hey1* mRNA levels in macrophages from DAPT-treated mice compared with those from vehicle control-treated mice (Fig. 7*B*). These data indicate that GSI treatment in vivo could inhibit Notch1 signaling activation in ALD-DNA–stimulated macrophages.

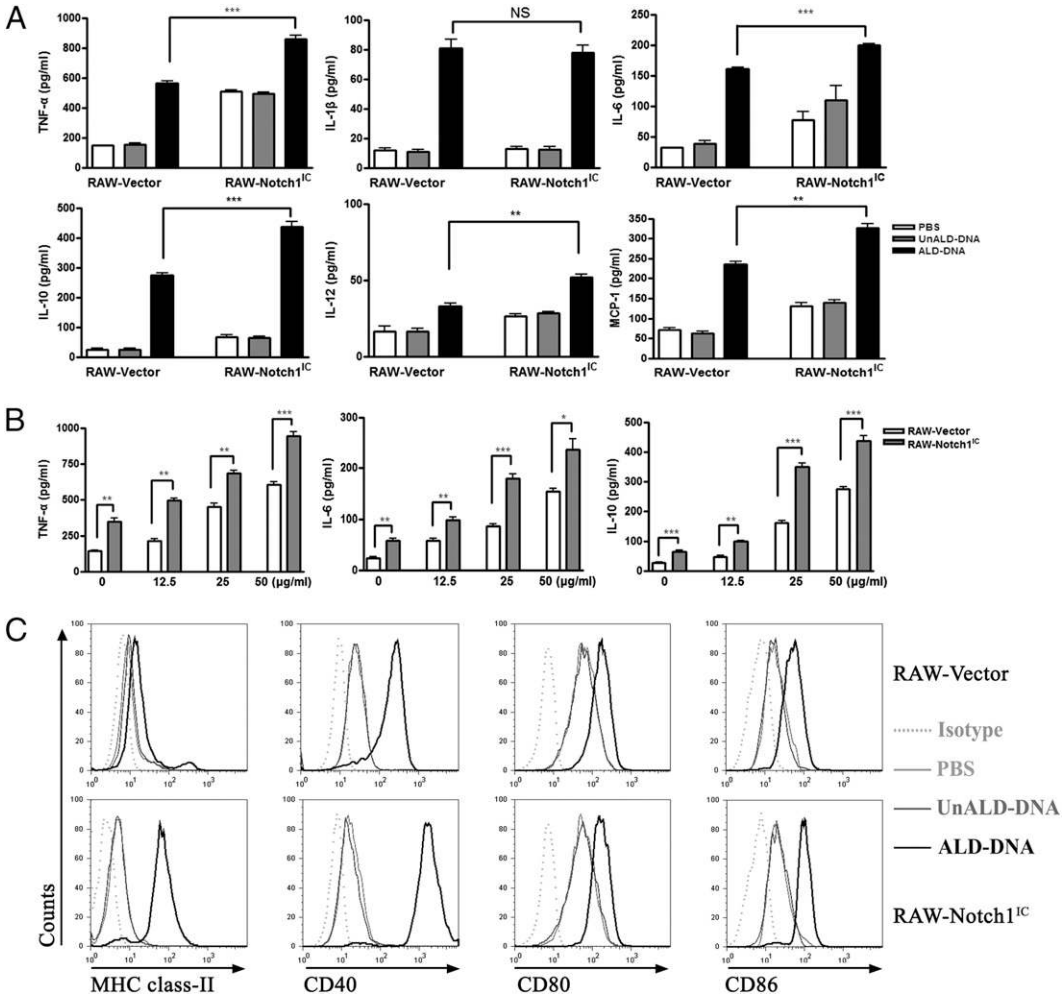

FIGURE 5. Notch1^{IC} overexpression promotes ALD-DNA–induced macrophage polarization. *A* and *C*, RAW-Vector and RAW-Notch1^{IC} cells were stimulated with ALD-DNA, UnALD-DNA, or PBS. *A*, Twelve hours poststimulation, expression levels of TNF-α, IL-1β, IL-6, IL-10, IL-12, and MCP-1 in the culture supernatants were measured by ELISA assay. *B*, RAW-Vector and RAW-Notch1^{IC} cells were stimulated with increasing amounts of ALD-DNA for 12 h, and cytokine expression levels of TNF-α, IL-6, and IL-10 in the culture supernatants were measured by ELISA assay. Data in *A* and *B* are means ± SD of three independent experiments. *C*, Twenty-four hours poststimulation, expression levels of MHC class II, CD40, CD80, and CD86 were assessed by flow cytometry analysis. Data are representative of results obtained in three independent experiments. $*p < 0.05$; $**p < 0.01$; $***p < 0.001$.

GSI treatment ameliorates SLE syndrome in the murine model by suppressing macrophage M2b polarization

To test the hypothesis that GSI treatment could ameliorate SLE syndrome in the murine model by inhibiting ALD-DNA–induced macrophage M2b polarization by suppressing Notch1 signaling activity, we firstly performed DAPT or vehicle control gavage treatment before the onset of nephritis in SLE mice. Decreased Notch1^{IC}, MHC class II, and CD86 protein levels and lower mRNA levels of the M2b phenotype markers were found in renal macrophages from DAPT-treated SLE mice versus those from vehicle control-treated SLE mice (Fig. 8*A*–*C*). To clarify the effect of decreased Notch1 signaling on macrophage Ag-presenting ability, we performed ELISA analysis for anti-dsDNA Ab production of B cells cocultured with macrophages from DAPT-treated mice combined with ALD-DNA induction. Anti-dsDNA Ab production of B cells was severely decreased by coculturing with macrophages from DAPT-treated SLE mice compared with those from vehicle control-treated SLE mice (Fig. 8*D*). Furthermore, ELISA analysis showed no change of anti-dsDNA IgG isotype, but decreased the concentration and avidity of anti-dsDNA IgG in serum from DAPT-treated SLE mice as compared with those from vehicle control-treated SLE mice (Fig. 8*E*–*G*). To examine the therapeutic effect of DAPT treatment on SLE syndrome in the murine model, we evaluated glomerulonephritis using urine protein quantification, renal tissue H&E staining, and autoantibody deposition analysis. More importantly, remarkably decreased urine protein, ameliorated glomerulonephritis, and reduced autoantibody deposition were found in DAPT-treated SLE mice compared with those of vehicle control-treated SLE mice (Fig. 8*H*–*K*). These data demonstrate that GSI treatment could prevent the onset of nephritis in the murine model through blunting of ALD-DNA–induced macrophage M2b polarization.

To further elucidate the effect of Notch inhibitor on activated macrophages and established SLE syndrome, we performed DAPT or vehicle control gavage treatment in SLE mice that already had produced autoantibody and developed proteinuria. Decreased Notch1^{IC} protein level and blunted M2b polarization were found in renal macrophages from DAPT-treated SLE mice versus those from vehicle control-treated SLE mice (Fig. 9*A*–*D*). More importantly, promptly decreased urine protein (Fig. 9*H*) and ameliorated glomerulonephritis (Fig. 9*I*, 9*J*) but tardily reduced autoantibody titers (Fig. 9*E*, 9*F*) and no notable changes of anti-dsDNA IgG avidity (Fig. 9*G*), IgG isotype (Fig. 9*E*), or autoantibody deposition (Fig. 9*K*) were found in DAPT-treated SLE mice

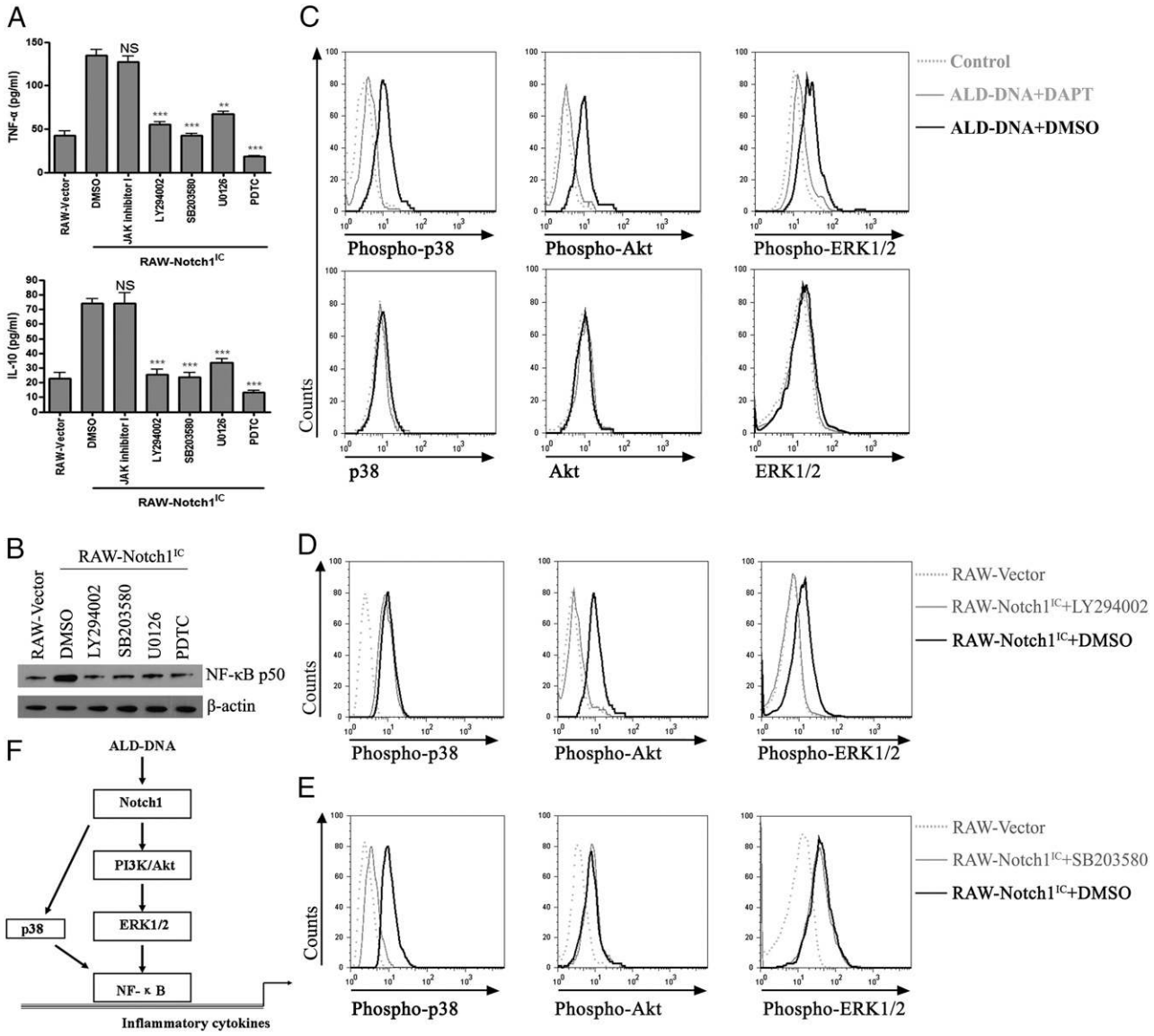

FIGURE 6. Notch1^{IC} facilitates macrophage M2b polarization through PI3K/Akt-ERK1/2 and P38 MAPK signaling pathways. *A*, RAW-Notch1^{IC} cells were treated with LY294002 (50 μM), SB203580 (10 μM), U0126 (10 μM), PDTC (50 μM), JAK inhibitor I (5 μM), or DMSO (0.1%) for 12 h. Cytokine expression levels of TNF-α and IL-10 in the culture supernatants of the RAW-Notch1^{IC} cells were determined by ELISA assay. RAW-Vector cells served as a control. Data are means ± SD of three independent experiments. *B*, RAW-Notch1^{IC} cells were treated with LY294002 (50 μM), SB203580 (10 μM), U0126 (10 μM), PDTC (50 μM), or DMSO (0.1%) for 1 h. Protein levels of NF-κB p50 in the nuclear extracts of RAW-Notch1^{IC} cells were analyzed by Western blot analysis. RAW-Vector cells served as a control. *C*, RAW264.7 cells were treated with DAPT (10 μM) or DMSO (0.1%) for 1 h and then stimulated with ALD-DNA for 1 h. The expression and phosphorylation levels of p38, Akt, and ERK1/2 in RAW264.7 cells were determined by flow cytometry analysis. *D* and *E*, Protein levels of phospho-p38, phospho-Akt, and phospho-ERK1/2 in RAW-Notch1^{IC} cells treated with LY294002 (50 μM), SB203580 (10 μM), or DMSO (0.1%) for 1 h were evaluated by flow cytometry analysis. RAW-Vector cells served as a control. *F*, Schematic representation of the molecular mechanism for ALD-DNA–induced macrophage activation. Data in *B–E* are representative of results obtained in three independent experiments. $^{**}p < 0.01$; $^{***}p < 0.001$.

compared with those of vehicle control-treated SLE mice. These data suggest that GSI treatment could induce remission of established nephritis in the SLE murine model by suppressing ALD-DNA–induced macrophage M2b polarization (Fig. 9*L*). In summary, these results demonstrate that GSI treatment could improve SLE syndrome in the murine model by blunting ALD-DNA–induced macrophage M2b polarization.

Discussion

It has been reported that individuals who are prone to the multisystem autoimmunity that is seen in patients with SLE might have uncharacterized defects in the ability of macrophages to clear apoptotic cells, thus providing immunogenic self-nuclear Ags derived from noningested apoptotic cells for undergoing secondary necrosis to supply for danger signals to the immune system, which indicates the association between self-nuclear Ags derived from apoptotic cells and autoimmunity in SLE (49–51). Further studies in knockout mice models revealed that lack of DNase I, serum amyloid P deficiency, or C1q absence resulted in exposure of redundant aberrant nucleic acid released from apoptotic cells to immune system, which could lead to antinuclear autoimmunity and SLE glomerulonephritis (52–55). Undigested DNA released from apoptotic cells could induce macrophage activation and trigger a set of immune response, thus producing autoantibodies to self-DNA, which occurs commonly in patients with SLE (6, 50). In this study, we used the SLE murine model established by our group previously by

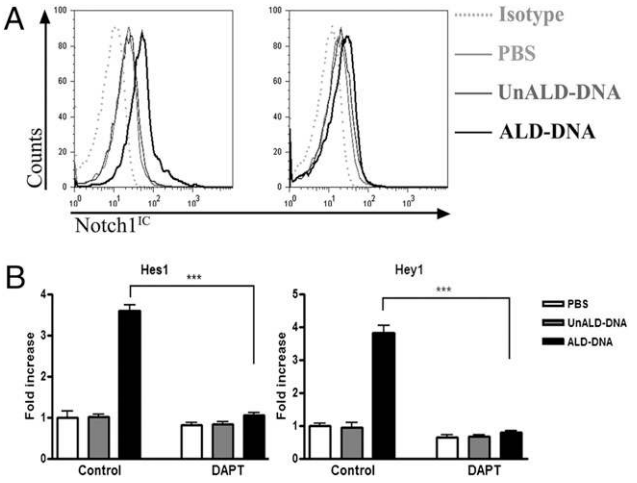

FIGURE 7. GSI treatment abrogates Notch1 signaling activity in ALD-DNA stimulated macrophages in vivo. Six- to 8-wk-old female BALB/c mice were treated with DAPT or vehicle control at 5 mg/kg per day for 4 d. Purified renal macrophages isolated from the mice were stimulated with ALD-DNA, UnALD-DNA, or PBS. *A*, Twenty-four hours poststimulation, expression levels of Notch1^{IC} were assessed by flow cytometry. Data are representative of results obtained in three independent experiments with renal macrophages from five mice in each group. *B*, Twelve hours poststimulation, mRNA levels of *Hes1* and *Hey1* were determined by real-time PCR analysis. Data are means ± SD of three independent experiments. $n = 5$. $^{***}p < 0.001$.

immunizing syngeneic female BALB/c mice with a self-DNA released from apoptotic lymphocytes that were termed ALD-DNA (9, 10). A series of SLE syndromes including highly anti-dsDNA Abs, proteinuria, and glomerulonephritis were developed in our murine model, which resembles human SLE syndrome accompanied by abundant self-DNA released from unremoved apoptotic cells. Thereby, the ALD-DNA–immunized mice could be used as an ideal murine lupus model to explore the potential cellular and molecular immunological mechanisms responsible for SLE disease.

There is considerable evidence that innate immune response performed mainly by activated macrophages and other myeloid cells triggered lupus autoimmune disease in both RAG-1–deficient moth-eaten mice and α-mannosidase-II–deficient mice, which indicated an important role of macrophage activation in the pathogenesis of SLE (13, 14, 56). Experimental data derived from NZB/W F_1 mice and Bcl2/11$^{-/-}$Fas$^{lpr/lpr}$ mice indicated that activated renal macrophages were characteristic markers of lupus nephritis in the SLE murine model, which further suggested the close association between macrophage activation and SLE pathogenesis (11, 15). In the current study, we demonstrated that macrophages induced by ALD-DNA were activated and polarized toward an M2b phenotype that could effectively trigger innate and adaptive immune response to self-DNA, thus leading to autoimmune response and tissue damage in the SLE murine model. We provided several lines of evidence that supported this notion. First, the nephritic tissues of SLE mice were found infiltrated with activated M2b-polarized macrophages. Secondly, ALD-DNA could induce macrophage activation and M2b polarization in vitro and in vivo. More importantly, blunted macrophage activation and M2b polarization through GSI treatment could decrease autoimmune responses and mitigate SLE syndrome in the murine model. We also found that macrophages depleting at the initial stage or a late stage of SLE disease protected mice against ALD-DNA–induced SLE syndrome in vivo (W. Zhang and S. Xiong, unpublished observations). All these results demonstrate that macrophage activation and M2b polarization could effectively drive ALD-DNA–induced autoimmunity and SLE syndrome. However, the plasticity of macrophages makes the task of assigning a particular phenotype to a particular population of macrophages with specific biochemical markers difficult (20). The phenotype of renal macrophages isolated in vivo and macrophages stimulated by ALD-DNA in vitro in this study might be flexible. Relative levels of infiltration by inflammatory and alternatively activated macrophages might change over time during the inflammatory process, and these macrophage subtypes might coexist in nephritis of SLE mice, which needs further investigation. The concrete DNA sensor in macrophages recognizing ALD-DNA also requires further elucidation.

Cell-cell signaling mediated by the Notch receptors is iteratively involved in a wide variety of developmental processes including the development and differentiation of immune system (29, 57). Apart from investigations on the contribution of Notch signaling to T/B cell lineage specification, Th cell differentiation, and DC differentiation and survival, increasing studies have been focused on the role of Notch signaling in the regulation of macrophage activation and function (58–63). In macrophages, TLR ligands have been reported to activate the canonical Notch signaling pathway as well as the well-known pathways of NF-κB p65 and p50 subunits, IRF3, IRF5, IRF7, and fos and jun pathways (32–34, 64). It is best characterized that the activation of NF-κB and other signaling pathways results in increased inflammatory cytokine expression including TNF-α, IL-10, IL-6, and IL-12 (64). Notch signaling has been reported to enhance cytokine expression through increasing NF-κB signaling activity and increasing Notch^{IC}-dependent RBPJ activation, which drives transcription of IL-6 directly (31). Meanwhile, Notch^{IC}-dependent RBPJ activation could also drive the Notch target genes *Hes1* and *Hey1*, which inhibits IL-6 and IL-12 expression but does not markedly alter TNF-α and IL-10 production (31). Therefore, these findings indicated that enhanced Notch signaling in macrophages might be involved in regulating the cytokine expression, which is associated with an M2b (type II) phenotype. We found that enhanced Notch1 signaling in macrophages stimulated with ALD-DNA in vitro and in vivo induced high levels of TNF-α, IL-6, and IL-10 but low levels of IL-12, which revealed that Notch1 signaling could promote macrophage M2b polarization. We also found that enhanced Notch1 signaling correlated with the elevated levels of MCP-1, which was reported to influence both innate immunity through effects on monocytes and adaptive immunity through control of Th2 polarization (65). Notably, TNF-α, IL-6, IL-10, and MCP-1, which could be induced by ALD-DNA, are elevated in the serum of patients with SLE and may contribute to the pathogenesis of SLE (66, 67). Our findings further demonstrated that Notch1 signaling could mediate macrophage M2b polarization in the SLE murine model, thus contributing to the pathogenesis of SLE. Although we could persistently detect the M2b macrophages in kidneys of SLE mice, we also found that in vitro ALD-DNA could induce macrophage M2b polarization following Notch1 signaling activation within 24 h. Alternative explanation for Notch1 pathway contributions in acute macrophage responses induced by ALD-DNA could not be excluded in this work. Interestingly, enhanced Notch1 signaling in macrophages stimulated by ALD-DNA was accompanied with increased NF-κB p50 translocation into nucleus, whereas GSI treatment strongly downregulated NF-κB activity. It has been shown that Notch signaling modulates NF-κB activity in macrophages and other cell types, which regulates the expression of several inflammatory cytokines and molecules responsible for Ag presentation (32, 68). The activation of PI3K and MAPK pathways also played key roles in Notch1 signaling-induced survival effects in many cell types (47). We found that Notch1 signaling

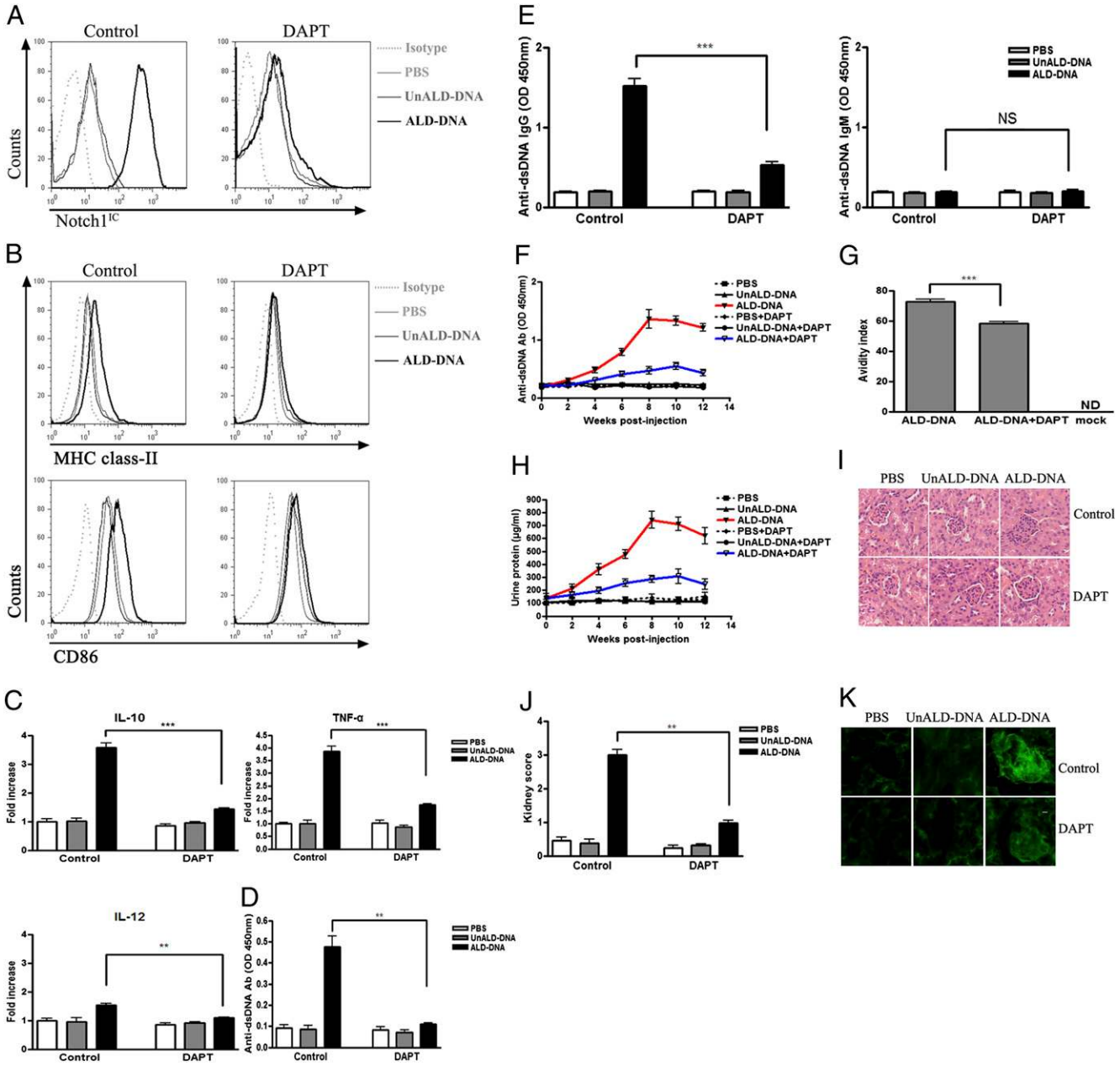

FIGURE 8. GSI treatment prevents SLE syndrome accompanied with decreased Notch1 signaling and blunted renal macrophage M2b polarization in the SLE mice. The mice were treated with DAPT or vehicle control by gavage for 3 mo. Twenty-four hours after the initial treatment, the mice were immunized with ALD-DNA, UnALD-DNA, or PBS three times in 4 wk. *A* and *B*, Eight weeks after initial immunization, expression levels of Notch1^{IC}, MHC class II, and CD86 in the renal macrophages from the mice were assessed by flow cytometry analysis. Data are representative of results obtained in three independent experiments with renal macrophages from four mice in each group. *C*, mRNA levels of *IL-10*, *TNF-α*, and *IL-12* in the renal macrophages purified from the mice were evaluated by real-time PCR. *D*, The purified renal macrophages from the DAPT-treated or control mice were cocultured with CD4$^+$ T cells and CD19$^+$ B cells from the SLE mice, then stimulated with ALD-DNA for 6 d. Levels of anti-dsDNA IgG in the culture supernatants were analyzed by ELISA. Data in *C* and *D* are means ± SD of three independent experiments. $n = 4$. The serum anti-dsDNA Ig levels at week 8 (*E*), serum anti-dsDNA IgG levels every 2 wk (*F*), and the avidity index of anti-dsDNA IgG at week 8 (*G*) were measured by ELISA. *H*, Urine protein levels of the mice were assessed by BCA Protein Assay kit (Thermo Fisher Scientific) every 2 wk. Data in *E*–*H* are means ± SD from 6–10 mice in each group. *I*, Eight weeks after initial immunization, nephritic pathological changes were shown by H&E staining of renal tissues surgical resected from the mice (original magnification ×200). Images are representative of at least 10 mice in each group. *J*, The kidney score was assessed using paraffin sections stained with H&E. *K*, Demonstration of IgG deposition in kidneys of the mice. Images are representative of at least 10 mice in each group (original magnification ×200). $^{**}p < 0.01$; $^{***}p < 0.001$.

accelerated NF-κB p50 translocation into the nucleus via PI3K and MAPK pathways in M2b-polarized macrophages induced by ALD-DNA. Based on these results, we demonstrated that Notch1 signaling could drive ALD-DNA–induced macrophage activation and M2b polarization by accelerating NF-κB p50 translocation into the nucleus via PI3K and MAPK pathways. Because Notch signaling activation is triggered by binding of Notch ligands with its receptors, whether enhanced Notch1 signaling in macrophages stimulated by ALD-DNA involves modulation of Notch1 ligands expression needs further study.

In our present study, significant activation of Notch1 signaling in ALD-DNA induced M2b-polarized macrophages, which was verified on mRNA and protein levels in vitro and in vivo. Furthermore, we demonstrated that Notch1 signaling contributed to

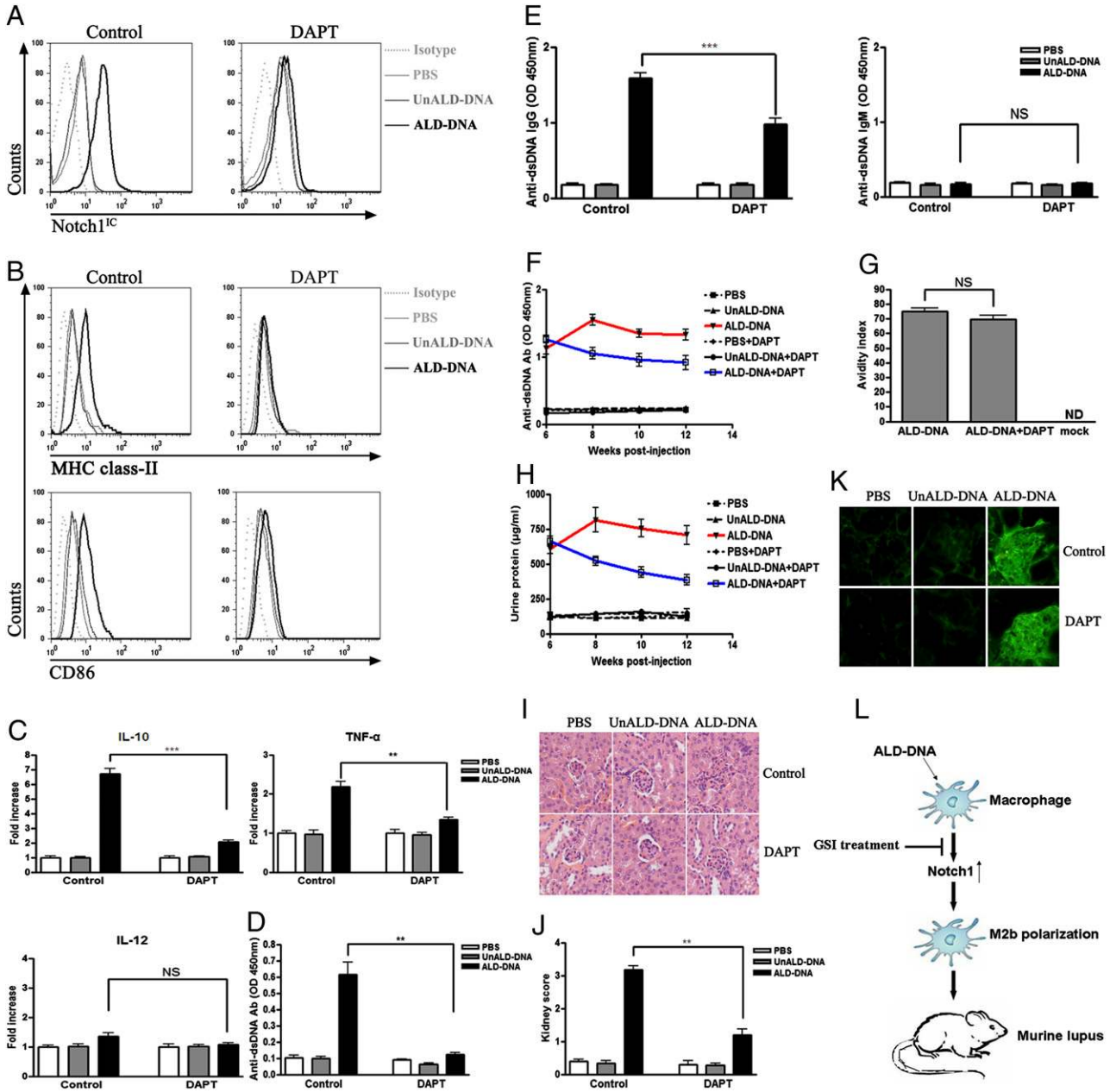

FIGURE 9. GSI treatment induces the remission of established nephritis accompanied with decreased Notch1 signaling and blunted renal macrophage M2b polarization in the SLE mice. The mice were immunized with ALD-DNA, UnALD-DNA, or PBS three times in 4 wk. Six weeks after initial immunization, the mice were treated with DAPT or vehicle control by gavage for another 6 wk. *A* and *B*, Twelve weeks after initial immunization, expression levels of Notch1^{IC}, MHC class II, and CD86 in the renal macrophages from the mice were assessed by flow cytometry analysis. Data are representative of results obtained in three independent experiments with renal macrophages from four mice in each group. *C*, mRNA levels of *IL-10*, *TNF-α*, and *IL-12* in the renal macrophages purified from the mice were evaluated by real-time PCR. *D*, The purified renal macrophages from the DAPT-treated or control mice were cocultured with CD4$^+$ T cells and CD19$^+$ B cells from the SLE mice, then stimulated with ALD-DNA for 6 d. Levels of anti-dsDNA IgG in the culture supernatants were analyzed by ELISA. Data in *C* and *D* are means ± SD of three independent experiments. $n = 4$. The serum anti-dsDNA Ig levels at week 12 (*E*), the serum anti-dsDNA IgG levels every 2 wk (*F*), and the avidity index of anti-dsDNA IgG at week 12 (*G*) were measured by ELISA. *H*, Urine protein levels of the mice were assessed by BCA Protein Assay Kit (Thermo Fisher Scientific) every 2 wk. Data in *E*–*H* are means ± SD from 6–10 mice in each group. *I*, Twelve weeks after initial immunization, nephritic pathological changes were shown by H&E staining of renal tissues surgical resected from the mice (original magnification ×200). Images are representative of at least 10 mice in each group. *J*, The kidney score was assessed using paraffin sections stained with H&E. *K*, Demonstration of IgG deposition in kidneys of the mice. Imagines are representative of at least 10 mice in each group (original magnification ×200). *L*, Schematic model for the role of Notch1 signaling-dependent M2b polarization in the pathogenesis of SLE syndrome induced by ALD-DNA. $^{**}p < 0.01$; $^{***}p < 0.001$.

ALD-DNA–induced macrophage polarization through inhibition of Notch1 signaling by GSI treatment and increased Notch1 signaling by Notch1^{IC} overexpression. More importantly, we found that the inhibition of Notch1 signaling by GSI treatment could attenuate SLE syndrome by suppressing ALD-DNA–induced macrophage M2b polarization in our murine model. Moreover, in the SLE mice treated with GSI as preventive therapy, macrophage activation and M2b polarization was blunted and accompanied by the ameliorated nephritis, decreased anti-dsDNA autoantibody, and no autoantibody deposition in the kidney. In addition to previous

reports about the effect of Notch1 signaling on the differentiation and activation of T/B cells, our present study raises the possibility that Notch1 signaling could also participate in the regulation of macrophage activation in the SLE mice. Compared with DAPT treatment in the initiation stage of SLE, DAPT treatment during the disease progression could also blunt macrophage M2b polarization and ameliorate glomerulonephritis but only slightly reduce autoantibody titers and autoantibody deposition in SLE mice. It is likely that GSI treatment could induce remission of established nephritis in the SLE murine model by suppressing macrophage M2b polarization, which might be induced by a mechanism downstream of renal autoantibody deposition (69, 70). Experimental data presented in this investigation demonstrated that Notch1 signaling activation involved in the pathogenesis of SLE syndrome through promotion of ALD-DNA–induced macrophage M2b polarization.

In summary, our present investigation demonstrates that contribution of elevated Notch1 signaling to ALD-DNA–induced macrophage M2b polarization, which plays a pivotal role in the pathogenesis of SLE syndrome, could be reversed by a specific GSI treatment, thus ameliorating SLE syndrome in the murine model. These innovative findings imply potently the possible development of new therapeutic strategies including GSI treatment for patients with SLE through blunted macrophage M2b polarization by blocking Notch1 activation.

Acknowledgments

We thank Prof. Tadatsugu Taniguchi for the gift of plasmids. We also thank Peng Hu, Cuini Wang, and Kang Li for technical assistance.

Disclosures

The authors have no financial conflicts of interest.

References

1. Rahman, A., and D. A. Isenberg. 2008. Systemic lupus erythematosus. *N. Engl. J. Med.* 358: 929–939.
2. Kotzin, B. L. 1996. Systemic lupus erythematosus. *Cell* 85: 303–306.
3. Teachey, D. T., A. E. Seif, V. I. Brown, M. Bruno, R. M. Bunte, Y. J. Chang, J. K. Choi, J. D. Fish, J. Hall, G. S. Reid, et al. 2008. Targeting Notch signaling in autoimmune and lymphoproliferative disease. *Blood* 111: 705–714.
4. Davidson, A., and B. Diamond. 2001. Autoimmune diseases. *N. Engl. J. Med.* 345: 340–350.
5. Desai, D. D., M. R. Krishnan, J. T. Swindle, and T. N. Marion. 1993. Antigen-specific induction of antibodies against native mammalian DNA in non-autoimmune mice. *J. Immunol.* 151: 1614–1626.
6. Vinuesa, C. G., and C. C. Goodnow. 2002. Immunology: DNA drives autoimmunity. *Nature* 416: 595–598.
7. Pisetsky, D. S. 1996. The immunologic properties of DNA. *J. Immunol.* 156: 421–423.
8. Leadbetter, E. A., I. R. Rifkin, A. M. Hohlbaum, B. C. Beaudette, M. J. Shlomchik, and A. Marshak-Rothstein. 2002. Chromatin-IgG complexes activate B cells by dual engagement of IgM and Toll-like receptors. *Nature* 416: 603–607.
9. Qiao, B., J. Wu, Y. W. Chu, Y. Wang, D. P. Wang, H. S. Wu, and S. D. Xiong. 2005. Induction of systemic lupus erythematosus-like syndrome in syngeneic mice by immunization with activated lymphocyte-derived DNA. *Rheumatology (Oxford)* 44: 1108–1114.
10. Wen, Z. K., W. Xu, L. Xu, Q. H. Cao, Y. Wang, Y. W. Chu, and S. D. Xiong. 2007. DNA hypomethylation is crucial for apoptotic DNA to induce systemic lupus erythematosus-like autoimmune disease in SLE-non-susceptible mice. *Rheumatology (Oxford)* 46: 1796–1803.
11. Schiffer, L., R. Bethunaickan, M. Ramanujam, W. Huang, M. Schiffer, H. Tao, M. P. Madaio, M. M. Madaio, E. P. Bottinger, and A. Davidson. 2008. Activated renal macrophages are markers of disease onset and disease remission in lupus nephritis. [Published erratum in 2008. *J. Immunol.* 180: 3613.] *J. Immunol.* 180: 1938–1947.
12. Liu, K., and C. Mohan. 2006. What do mouse models teach us about human SLE? *Clin. Immunol.* 119: 123–130.
13. Paulson, J. C. 2007. Innate immune response triggers lupus-like autoimmune disease. *Cell* 130: 589–591.
14. Green, R. S., E. L. Stone, M. Tenno, E. Lehtonen, M. G. Farquhar, and J. D. Marth. 2007. Mammalian N-glycan branching protects against innate immune self-recognition and inflammation in autoimmune disease pathogenesis. *Immunity* 27: 308–320.
15. Hutcheson, J., J. C. Scatizzi, A. M. Siddiqui, G. K. Haines, 3rd, T. Wu, Q. Z. Li, L. S. Davis, C. Mohan, and H. Perlman. 2008. Combined deficiency of proapoptotic regulators Bim and Fas results in the early onset of systemic autoimmunity. *Immunity* 28: 206–217.
16. Hill, G. S., M. Delahousse, D. Nochy, P. Rémy, F. Mignon, J. P. Méry, and J. Bariéty. 2001. Predictive power of the second renal biopsy in lupus nephritis: significance of macrophages. *Kidney Int.* 59: 304–316.
17. Jothy, S., and R. J. Sawka. 1981. Presence of monocytes in systemic lupus erythematosus-associated glomerulonephritis: marker study and significance. *Arch. Pathol. Lab. Med.* 105: 590–593.
18. Kobayashi, M., A. Koyama, M. Narita, and H. Shigematsu. 1991. Intraglomerular monocytes in human glomerulonephritis. *Nephron* 59: 580–585.
19. Lan, H. Y., D. J. Nikolic-Paterson, W. Mu, and R. C. Atkins. 1995. Local macrophage proliferation in the progression of glomerular and tubulointerstitial injury in rat anti-GBM glomerulonephritis. *Kidney Int.* 48: 753–760.
20. Mosser, D. M., and J. P. Edwards. 2008. Exploring the full spectrum of macrophage activation. *Nat. Rev. Immunol.* 8: 958–969.
21. Mantovani, A., A. Sica, and M. Locati. 2005. Macrophage polarization comes of age. *Immunity* 23: 344–346.
22. Benoit, M., B. Desnues, and J. L. Mege. 2008. Macrophage polarization in bacterial infections. *J. Immunol.* 181: 3733–3739.
23. Martinez, F. O., L. Helming, and S. Gordon. 2009. Alternative activation of macrophages: an immunologic functional perspective. *Annu. Rev. Immunol.* 27: 451–483.
24. Mantovani, A., A. Sica, S. Sozzani, P. Allavena, A. Vecchi, and M. Locati. 2004. The chemokine system in diverse forms of macrophage activation and polarization. *Trends Immunol.* 25: 677–686.
25. Li, K., W. Xu, Q. Guo, Z. Jiang, P. Wang, Y. Yue, and S. Xiong. 2009. Differential macrophage polarization in male and female BALB/c mice infected with coxsackievirus B3 defines susceptibility to viral myocarditis. *Circ. Res.* 105: 353–364.
26. Gordon, S. 2003. Alternative activation of macrophages. *Nat. Rev. Immunol.* 3: 23–35.
27. Artavanis-Tsakonas, S., M. D. Rand, and R. J. Lake. 1999. Notch signaling: cell fate control and signal integration in development. *Science* 284: 770–776.
28. Maillard, I., T. Fang, and W. S. Pear. 2005. Regulation of lymphoid development, differentiation, and function by the Notch pathway. *Annu. Rev. Immunol.* 23: 945–974.
29. Tanigaki, K., and T. Honjo. 2007. Regulation of lymphocyte development by Notch signaling. *Nat. Immunol.* 8: 451–456.
30. Ohishi, K., B. Varnum-Finney, R. E. Serda, C. Anasetti, and I. D. Bernstein. 2001. The Notch ligand, Delta-1, inhibits the differentiation of monocytes into macrophages but permits their differentiation into dendritic cells. *Blood* 98: 1402–1407.
31. Hu, X., A. Y. Chung, I. Wu, J. Foldi, J. Chen, J. D. Ji, T. Tateya, Y. J. Kang, J. Han, M. Gessler, et al. 2008. Integrated regulation of Toll-like receptor responses by Notch and interferon-gamma pathways. *Immunity* 29: 691–703.
32. Palaga, T., C. Buranaruk, S. Rengpipat, A. H. Fauq, T. E. Golde, S. H. Kaufmann, and B. A. Osborne. 2008. Notch signaling is activated by TLR stimulation and regulates macrophage functions. *Eur. J. Immunol.* 38: 174–183.
33. Narayana, Y., and K. N. Balaji. 2008. NOTCH1 up-regulation and signaling involved in *Mycobacterium* bovis BCG-induced SOCS3 expression in macrophages. *J. Biol. Chem.* 283: 12501–12511.
34. Monsalve, E., M. A. Pérez, A. Rubio, M. J. Ruiz-Hidalgo, V. Baladrón, J. J. García-Ramírez, J. C. Gómez, J. Laborda, and M. J. Díaz-Guerra. 2006. Notch-1 up-regulation and signaling following macrophage activation modulates gene expression patterns known to affect antigen-presenting capacity and cytotoxic activity. *J. Immunol.* 176: 5362–5373.
35. Ito, T., M. Schaller, C. M. Hogaboam, T. J. Standiford, M. Sandor, N. W. Lukacs, S. W. Chensue, and S. L. Kunkel. 2009. TLR9 regulates the mycobacteria-elicited pulmonary granulomatous immune response in mice through DC-derived Notch ligand delta-like 4. *J. Clin. Invest.* 119: 33–46.
36. Sato, M., H. Suemori, N. Hata, M. Asagiri, K. Ogasawara, K. Nakao, T. Nakaya, M. Katsuki, S. Noguchi, N. Tanaka, and T. Taniguchi. 2000. Distinct and essential roles of transcription factors IRF-3 and IRF-7 in response to viruses for IFN-alpha/beta gene induction. *Immunity* 13: 539–548.
37. Takaoka, A., H. Yanai, S. Kondo, G. Duncan, H. Negishi, T. Mizutani, S. Kano, K. Honda, Y. Ohba, T. W. Mak, and T. Taniguchi. 2005. Integral role of IRF-5 in the gene induction programme activated by Toll-like receptors. *Nature* 434: 243–249.
38. Capozzo, A. V., K. Ramírez, J. M. Polo, J. Ulmer, E. M. Barry, M. M. Levine, and M. F. Pasetti. 2006. Neonatal immunization with a Sindbis virus-DNA measles vaccine induces adult-like neutralizing antibodies and cell-mediated immunity in the presence of maternal antibodies. *J. Immunol.* 176: 5671–5681.
39. Perez, O. D., and G. P. Nolan. 2002. Simultaneous measurement of multiple active kinase states using polychromatic flow cytometry. *Nat. Biotechnol.* 20: 155–162.
40. Lumeng, C. N., J. L. Bodzin, and A. R. Saltiel. 2007. Obesity induces a phenotypic switch in adipose tissue macrophage polarization. *J. Clin. Invest.* 117: 175–184.
41. Gao, B., Z. Duan, W. Xu, and S. Xiong. 2009. Tripartite motif-containing 22 inhibits the activity of hepatitis B virus core promoter, which is dependent on nuclear-located RING domain. *Hepatology* 50: 424–433.
42. Minhajuddin, M., F. Fazal, K. M. Bijli, M. R. Amin, and A. Rahman. 2005. Inhibition of mammalian target of rapamycin potentiates thrombin-induced intercellular adhesion molecule-1 expression by accelerating and stabilizing NF-kappa B activation in endothelial cells. *J. Immunol.* 174: 5823–5829.

43. Chung, E. Y., J. Liu, Y. Homma, Y. Zhang, A. Brendolan, M. Saggese, J. Han, R. Silverstein, L. Selleri, and X. Ma. 2007. Interleukin-10 expression in macrophages during phagocytosis of apoptotic cells is mediated by homeodomain proteins Pbx1 and Prep-1. *Immunity* 27: 952–964.
44. Guan, E., J. Wang, J. Laborda, M. Norcross, P. A. Baeuerle, and T. Hoffman. 1996. T cell leukemia-associated human Notch/translocation-associated Notch homologue has I kappa B-like activity and physically interacts with nuclear factor-kappa B proteins in T cells. *J. Exp. Med.* 183: 2025–2032.
45. Rosati, E., R. Sabatini, G. Rampino, A. Tabilio, M. Di Ianni, K. Fettucciari, A. Bartoli, S. Coaccioli, I. Screpanti, and P. Marconi. 2009. Constitutively activated Notch signaling is involved in survival and apoptosis resistance of B-CLL cells. *Blood* 113: 856–865.
46. McKenzie, G., G. Ward, Y. Stallwood, E. Briend, S. Papadia, A. Lennard, M. Turner, B. Champion, and G. E. Hardingham. 2006. Cellular Notch responsiveness is defined by phosphoinositide 3-kinase-dependent signals. *BMC Cell Biol.* 7: 10.
47. Liu, Z. J., M. Xiao, K. Balint, K. S. Smalley, P. Brafford, R. Qiu, C. C. Pinnix, X. Li, and M. Herlyn. 2006. Notch1 signaling promotes primary melanoma progression by activating mitogen-activated protein kinase/phosphatidylinositol 3-kinase-Akt pathways and up-regulating N-cadherin expression. *Cancer Res.* 66: 4182–4190.
48. Sade, H., S. Krishna, and A. Sarin. 2004. The anti-apoptotic effect of Notch-1 requires p56lck-dependent, Akt/PKB-mediated signaling in T cells. *J. Biol. Chem.* 279: 2937–2944.
49. Savill, J., I. Dransfield, C. Gregory, and C. Haslett. 2002. A blast from the past: clearance of apoptotic cells regulates immune responses. *Nat. Rev. Immunol.* 2: 965–975.
50. Okabe, Y., K. Kawane, S. Akira, T. Taniguchi, and S. Nagata. 2005. Toll-like receptor-independent gene induction program activated by mammalian DNA escaped from apoptotic DNA degradation. *J. Exp. Med.* 202: 1333–1339.
51. Mukundan, L., J. I. Odegaard, C. R. Morel, J. E. Heredia, J. W. Mwangi, R. R. Ricardo-Gonzalez, Y. P. Goh, A. R. Eagle, S. E. Dunn, J. U. Awakuni, et al. 2009. PPAR-delta senses and orchestrates clearance of apoptotic cells to promote tolerance. *Nat. Med.* 15: 1266–1272.
52. Napirei, M., H. Karsunky, B. Zevnik, H. Stephan, H. G. Mannherz, and T. Möröy. 2000. Features of systemic lupus erythematosus in Dnase1-deficient mice. *Nat. Genet.* 25: 177–181.
53. Bickerstaff, M. C., M. Botto, W. L. Hutchinson, J. Herbert, G. A. Tennent, A. Bybee, D. A. Mitchell, H. T. Cook, P. J. Butler, M. J. Walport, and M. B. Pepys. 1999. Serum amyloid P component controls chromatin degradation and prevents antinuclear autoimmunity. *Nat. Med.* 5: 694–697.
54. Familian, A., B. Zwart, H. G. Huisman, I. Rensink, D. Roem, P. L. Hordijk, L. A. Aarden, and C. E. Hack. 2001. Chromatin-independent binding of serum amyloid P component to apoptotic cells. *J. Immunol.* 167: 647–654.
55. Botto, M., C. Dell'Agnola, A. E. Bygrave, E. M. Thompson, H. T. Cook, F. Petry, M. Loos, P. P. Pandolfi, and M. J. Walport. 1998. Homozygous C1q deficiency causes glomerulonephritis associated with multiple apoptotic bodies. *Nat. Genet.* 19: 56–59.
56. Yu, C. C., H. W. Tsui, B. Y. Ngan, M. J. Shulman, G. E. Wu, and F. W. Tsui. 1996. B and T cells are not required for the viable motheaten phenotype. *J. Exp. Med.* 183: 371–380.
57. Radtke, F., A. Wilson, S. J. Mancini, and H. R. MacDonald. 2004. Notch regulation of lymphocyte development and function. *Nat. Immunol.* 5: 247–253.
58. Besseyrias, V., E. Fiorini, L. J. Strobl, U. Zimber-Strobl, A. Dumortier, U. Koch, M. L. Arcangeli, S. Ezine, H. R. Macdonald, and F. Radtke. 2007. Hierarchy of Notch-Delta interactions promoting T cell lineage commitment and maturation. *J. Exp. Med.* 204: 331–343.
59. Jenkinson, E. J., W. E. Jenkinson, S. W. Rossi, and G. Anderson. 2006. The thymus and T-cell commitment: the right niche for Notch? *Nat. Rev. Immunol.* 6: 551–555.
60. Fang, T. C., Y. Yashiro-Ohtani, C. Del Bianco, D. M. Knoblock, S. C. Blacklow, and W. S. Pear. 2007. Notch directly regulates Gata3 expression during T helper 2 cell differentiation. *Immunity* 27: 100–110.
61. Tu, L., T. C. Fang, D. Artis, O. Shestova, S. E. Pross, I. Maillard, and W. S. Pear. 2005. Notch signaling is an important regulator of type 2 immunity. *J. Exp. Med.* 202: 1037–1042.
62. Caton, M. L., M. R. Smith-Raska, and B. Reizis. 2007. Notch-RBP-J signaling controls the homeostasis of CD8- dendritic cells in the spleen. *J. Exp. Med.* 204: 1653–1664.
63. Zhou, J., P. Cheng, J. I. Youn, M. J. Cotter, and D. I. Gabrilovich. 2009. Notch and wingless signaling cooperate in regulation of dendritic cell differentiation. *Immunity* 30: 845–859.
64. Hertzog, P. 2008. A notch in the toll belt. *Immunity* 29: 663–665.
65. Gu, L., S. Tseng, R. M. Horner, C. Tam, M. Loda, and B. J. Rollins. 2000. Control of TH2 polarization by the chemokine monocyte chemoattractant protein-1. *Nature* 404: 407–411.
66. Urbonaviciute, V., B. G. Fürnrohr, S. Meister, L. Munoz, P. Heyder, F. De Marchis, M. E. Bianchi, C. Kirschning, H. Wagner, A. A. Manfredi, et al. 2008. Induction of inflammatory and immune responses by HMGB1-nucleosome complexes: implications for the pathogenesis of SLE. *J. Exp. Med.* 205: 3007–3018.
67. Tesch, G. H., S. Maifert, A. Schwarting, B. J. Rollins, and V. R. Kelley. 1999. Monocyte chemoattractant protein 1-dependent leukocytic infiltrates are responsible for autoimmune disease in MRL-Fas(lpr) mice. *J. Exp. Med.* 190: 1813–1824.
68. Shin, H. M., L. M. Minter, O. H. Cho, S. Gottipati, A. H. Fauq, T. E. Golde, G. E. Sonenshein, and B. A. Osborne. 2006. Notch1 augments NF-kappaB activity by facilitating its nuclear retention. *EMBO J.* 25: 129–138.
69. Schiffer, L., J. Sinha, X. Wang, W. Huang, G. von Gersdorff, M. Schiffer, M. P. Madaio, A. Davidson, and G. Von Gonsdorff. 2003. Short term administration of costimulatory blockade and cyclophosphamide induces remission of systemic lupus erythematosus nephritis in NZB/W F1 mice by a mechanism downstream of renal immune complex deposition. [Published erratum in 2003 *J. Immunol.* 171: 1610.] *J. Immunol.* 171: 489–497.
70. Triantafyllopoulou, A., C. W. Franzke, S. V. Seshan, G. Perino, G. D. Kalliolias, M. Ramanujam, N. van Rooijen, A. Davidson, and L. B. Ivashkiv. 2010. Proliferative lesions and metalloproteinase activity in murine lupus nephritis mediated by type I interferons and macrophages. *Proc. Natl. Acad. Sci. U.S.A.* 107: 3012–3017.